

A convolution neural network model for knee osteoporosis classification using X-ray images

Omar Khalid M. Ali¹, Abeer K. Ibrahim², Bilal R. Altamer³

¹Department of Construction and Projects, Mosul University Presidency, University of Mosul, Mosul, Iraq

²Department of Environment Engineering, Faculty of Engineering, University of Mosul, Mosul, Iraq

³Department of Presidency Affairs, Mosul University Presidency, University of Mosul, Mosul, Iraq

Article Info

Article history:

Received Nov 12, 2024

Revised Mar 26, 2025

Accepted May 10, 2025

Keywords:

Accuracy

Convolutional neural networks

Knee osteoporosis

Osteopenia

X-ray

ABSTRACT

Bone structure deterioration along with low levels of bone density are the hallmarks of knee osteoporosis (KOP). The conventional approach for detecting osteoporosis is accomplished using a knee radiograph, but it requires specialized knowledge. Nevertheless, X-rays can be difficult to interpret due to their large volume and minor fluctuations. In the past few decades, deep learning algorithms have minimized misinterpretation and modified medical diagnosis. In particular, algorithms based on convolutional neural networks (CNNs) have been used to speed up the procedure of diagnosis because of their innate capacity to extract significant features that often are challenging to spot by hand. A robust CNN model was proposed in this paper for KOP classification which uses a train and test approach to recognize healthy, osteopenia-predicted, and osteoporosis knee cases using 1947 X-ray images. The proposed model was designed using Jupyter Notebook and is in Python. To verify the efficiency of the model, some factors were calculated such as accuracy, precision, recall, and f1-score. In comparison with other similar systems, the results obtained showed that the accuracy of the proposed system reached 90.25%.

This is an open access article under the [CC BY-SA](https://creativecommons.org/licenses/by-sa/4.0/) license.



Corresponding Author:

Omar Khalid M. Ali

Department of Construction and Projects, Mosul University Presidency, University of Mosul

Left side, Al-Baladiyat district, 41002, Mosul, Iraq

Email: omar.khalid@uomosul.edu.iq

1. INTRODUCTION

Osteoporosis is defined as a decrease in bone mass and the deterioration of bone cells, which lowers the density of bones and raises the possibility of bone fractures. Knee osteoporosis (KOP), a particular type of osteoporosis that mainly impacts the knee region and has been more well-known in the past few years, threatens countless people [1], [2]. The World Health Organization (WHO) has identified numerous important risk aspects for the growth of KOP, comprising family history, gender, age, hormone abnormalities, and habits such as extreme alcohol intake [3]–[5]. Common symptoms of this illness include decreased mobility, stiffness, and ongoing pain and discomfort in the knee area, each of which has a substantial negative impact on a person's lifestyle [3], [6]. It is crucial to remember that KOP is an incurable illness, but prompt diagnosis and targeted treatment can greatly reduce or even stop its course, enhancing the general health of those who are impacted [6].

In the medical field, osteoporosis is identified using the dual-energy X-ray absorptiometry technique (DXA) [7] which measures bone mineral density (BMD) according to the Z-score and T-score parameters that the WHO has approved for various phases of the disease [8]. Nevertheless, this approach has drawbacks, including areal measures, expense, and limited availability. Magnetic resonance imaging (MRI) [9], computed tomography (CT) [10], and the quantitative ultrasound system (QUS) [11], are other imaging techniques

utilized to identify osteoporosis. A detection system that is precise, affordable, and easily accessible is necessary in light of these constraints. Due to this requirement, scientists have been using computer algorithms to evaluate medical images and create computer-aided diagnostic systems (CAD) by utilizing current developments in imaging technologies. The advent of advanced imaging techniques and computational methods has ushered in new opportunities for the diagnosis and management of KOP. Traditional methods, while effective to some extent, often fall short in terms of accessibility and cost-efficiency. This gap has driven the development of CAD systems, which utilize machine learning and image processing techniques to provide more accurate and accessible diagnosis options [12]. Many experiments have shown that these AI-based systems may attain exceptional levels of precision, frequently surpassing conventional diagnostic approaches [11]. Once a model's decisions are completely understandable, it will be interpreted [13]. However, artificial intelligence models remain mysterious to average users. Therefore, a deeper comprehension of the models' operations becomes essential to set goals for a larger application of artificial intelligence technologies in medicine. As a result, efforts have been initiated to enhance artificial intelligence models' transparency and interpretability [14]. The following are several previous research findings provided by different scientists throughout the past several years.

Hatano *et al.* [15], Produced an automatic diagnosing system that includes three steps: segmentation, registration, and classification. Their approach worked well, with 92.89% true positives and 5.96% false positives achieved in the categorization rates. Hatano *et al.* [16], presented an automatic identification method of osteoporosis from phalanges computed radiography (CR) images using deep convolutional neural network (DCNN) and tested its effectiveness by a three-fold cross-validation approach. The authors use a DCNN classifier to determine if unknown CR images are normal or not. Fathima *et al.* [17], utilized an adjusted U-Net with a Concentration unit to segment the bone regions from Dual Energy X-ray Absorptiometry (DEXA) images and X-rays. The dataset was classified into three classes by computing T-score and BMD. The accuracy of the proposed method was about 88%. Zhang *et al.* [18], developed a model of DCNN for classifying osteoporosis and osteopenia based on the X-ray images of the lumbar spine. The developed model was assessed by measuring the T-score factor and then classifying the dataset into three classes: normal, osteoporosis, and osteopenia. Teclé *et al.* [19], compared human and machine osteoporosis diagnoses using a second metacarpal cortical percentage. The results indicate that the Sensitivity was 82.4%, and the Specificity was 94.3%. Ho *et al.* [20], proposed a deep learning approach that can accurately predict the density of bone minerals gathered from a plain pelvic X-ray for osteoporosis classifying. Their technique combines convolutional neural network (CNN) learning, image segmentation, and (DeepDXA) which is a convolution model to estimate bone minerals data value by connecting separated femur bone images. In this paper, a CNN model-based KOP detection and classification is proposed. The main goal of this work is to enhance the concept of diagnosis through AI by obtaining high diagnostic accuracy.

2. METHOD

First of all, the knee X-ray dataset available on the Kaggle website is utilized [21]. Figures 1(a) to (c) illustrate examples of the used datasets, which consist of 1947 images with 3 classes: healthy, actual osteopenia, and osteoporosis. Next, these datasets are split into two parts, the first is concerned with training the CNN model, and the second is concerned with test data (which the trained classifier is tested with) with validation for each epoch. Since CNN performs better with additional data, the training collection's image count is increased by augmenting the training data. After that, the CNN model receives this collection of images in order to be trained. Eventually, the prediction proportion of both test and train data is assessed, and the classifier's efficiency in classifying images into osteoporosis, osteopenia, and normal images is estimated.

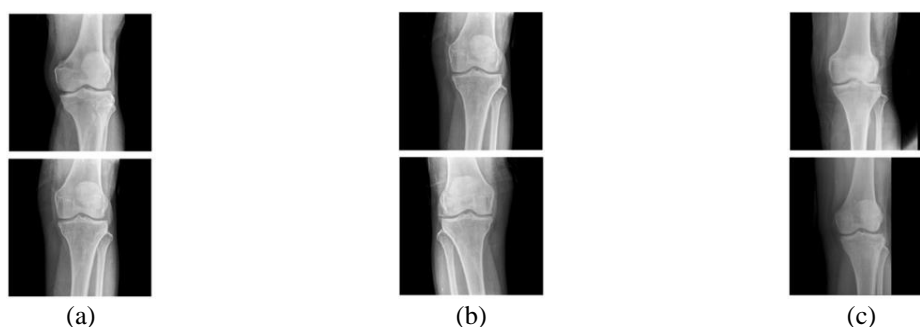


Figure 1. Samples of the used dataset; (a) healthy, (b) osteopenia predicted, and (c) osteoporosis

Figure 2 demonstrates the suggested block diagram model for detecting osteoporosis via knee X-rays. In this proposed CNN model, the rectified linear unit (ReLU) is utilized after each convolution layer and all fully connected (FC) layers, with the exception of the final FC layer. When CNN uses the ReLU function, it trains much more quickly than when it uses alternative activation functions like sigmoid or Tanh functions [22]. The mathematical expression of the ReLU activation function is demonstrated in (1) [23].

$$f(x) = \max(0; x) \quad (1)$$

The optimal CNN structure created using the suggested algorithm involves nine convolution steps, four pooling steps, three dense steps, and two dropout steps, as shown in Table 1. In addition, the architecture of the proposed CNN model has 15,610,499 total parameters, 15,604,099 trainable parameters, and 6,400 non-trainable parameters. The value of the loss function was calculated using categorical cross-entropy, and the network's trainable parameters were then modified to reduce prediction loss.

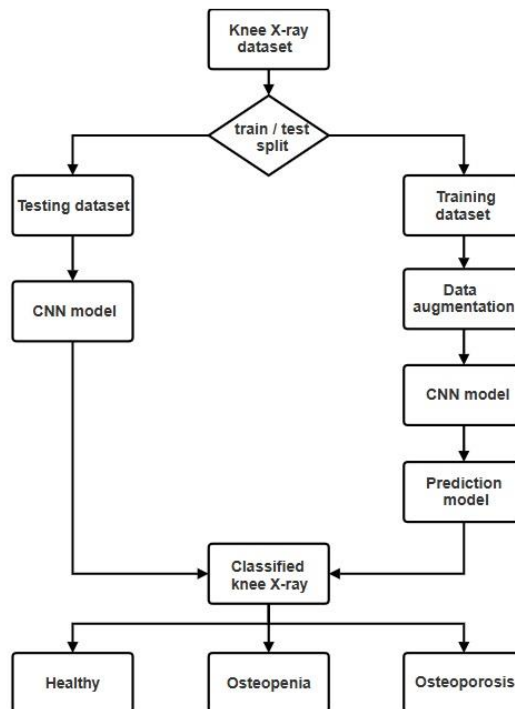


Figure 2. The block diagram of the proposed CNN model

Table 1. The proposed CNN model design and parameters

Layer (type)	No. of kernel	Kernel size	Output shape	No. of parameters
Conv1(Conv2D)	128	(8, 8)	(73, 73, 128)	24704
Conv2(Conv2D)	256	(5, 5)	(73, 73, 256)	819456
Pooling1(MaxPooling2D)	-	(3, 3)	(24, 24, 256)	0
Conv3(Conv2D)	256	(3, 3)	(24, 24, 256)	590080
Conv4(Conv2D)	256	(1, 1)	(24, 24, 256)	65792
Conv5(Conv2D)	256	(1, 1)	(24, 24, 256)	65792
Conv6(Conv2D)	512	(3, 3)	(24, 24, 512)	1180160
Pooling2(MaxPooling2D)	-	(2, 2)	(12, 12, 512)	0
Conv7(Conv2D)	512	(3, 3)	(12, 12, 512)	2359808
Conv8(Conv2D)	512	(3, 3)	(12, 12, 512)	2359808
Pooling3(MaxPooling2D)	-	(2, 2)	(6, 6, 512)	0
Conv9(Conv2D)	512	(3, 3)	(6, 6, 512)	2359808
Pooling4(MaxPooling2D)	-	(2, 2)	(3, 3, 512)	0
Flatten(Flatten)	-	-	4609	0
Dense1(Dense)	-	-	1024	4719616
Drop1(Dropout)	-	-	1024	0
Dense2(Dense)	-	-	1024	1049600
Drop2(Dropout)	-	-	1024	0
Dense3(Dense)	-	-	3	3075

2.1. Convolutional neural network architecture

CNN is a kind of neural network with deep layers that utilize the convolution principle at its stage of development. The computational function known as convolution is used to combine two functions to create a novel one with altered properties [24]. CNNs are employed to analyze images that have been convolved using a filter that is smaller in length than in width to minimize the image size while preserving the essential information. Scientists are more interested in CNN than other machine learning systems because it can take advantage of the simultaneous spatial and configurational information of both 2D and 3D images [25].

CNN's strength lies in its ability to extract features directly from images, unlike other machine-learning techniques that need object segmentation [26] or feature extraction [27]. Numerous CNNs have been created to address different kinds of issues; while they differ slightly from one another in certain areas, all of their fundamental elements remain the same. The CNNs involve three kinds of layers: convolutional layer, pooling layer, and fully connected layer [28], as demonstrated in Figure 3.

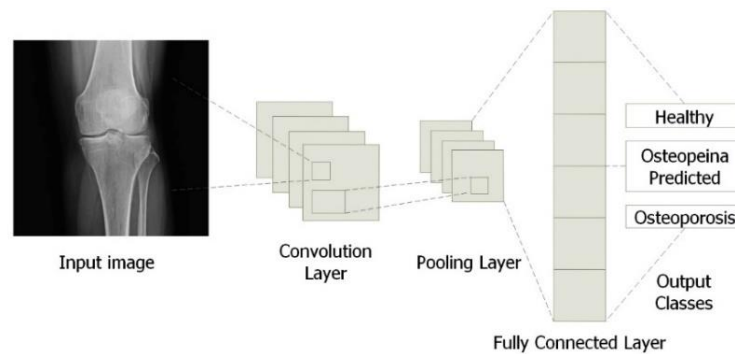


Figure 3. The CNN architecture

2.2. Convolution layer

The convolution layer is considered the most significant layer that makes up convolutional neural networks and is founded on continuously circulating a specific filter across the whole image. In a nutshell, the image pixel values are multiplied by the kernel frame by dragging it right or left across the image being processed or the image of the prior layer. When the filter or kernel reaches the matrix's border, it is moved down within the required unit, and identical processes are carried out. Then, a feature matrix or a more accurate feature map is produced once the whole image has been processed. This feature map shows the locations of features unique for every filter. The (2) illustrates the mathematical representation of the convolution process [29].

$$S(i, j) = (I * K)(i, j) = \sum_m \sum_n I(i + m, j + n) K(m, n) \quad (2)$$

where: * represents the convolution process, S describes the result of convolution, I refer to the input, and K refers to the kernel.

At a convolutional layer, several feature matrices are added to either the input image or the output matrices from the preceding layer. These feature matrices allow for parameter training and updating each row and column based on the propagated gradient values after every training cycle. The weights in this layer can be shared by employing similar filters into the identical feature map, resulting in a significantly decreased overall number of parameters for the neural network. Several critical parameters in this layer such as filter number, filter width, padding, and stride are specified by developers [22]. The overall filter dimensions utilized in convolution operations are typically odd, allowing the filter to have a central point and offer asymmetrical padding. Whereas the kernel matrix is moving across the image, the stride (with a shift quantity) parameter controls the amount that it changes in every step. In contrast, padding involves adding zero evenly to a given input matrix in order to preserve a dimension of the output matrices equal to that of the input [30]. An example of the convolution process using a (4×4) input image, (3×3) convolution core, and (1) stride is displayed in Figure 4.

To obtain the appropriate feature maps, different attributes are found utilizing various kernels and repeated. Behind convolution, the resulting image's size is computed as (3) [31]:

$$\text{output matrix dimension} = \frac{\text{input size} + 2 \text{ padding} - \text{kernel size}}{\text{stride}} + 1 \quad (3)$$

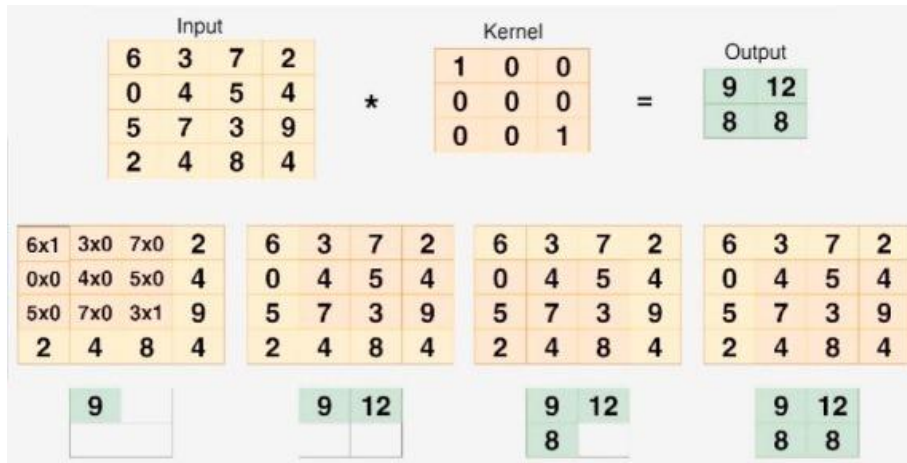


Figure 4. Example of convolution process [31]

2.3. Pooling layer

As for the pooling layer, it decreases the extent of the features gathered from the preceding layer, and identical features become more prominent. It accomplishes this by rearranging the image's specified filters. Stated otherwise, it executes the subsampling procedure. Consequently, the following layer's data size will decrease, and the resulting model won't overfit. It is vital to remember that this drop results in the disappearance of some crucial data. The main advantage of the pooling layer is that it reduces the number of factors that the neural network must estimate, which lowers the network's computational difficulty and speeds up training [32]. A pooling procedure is achieved in three forms, minimum pooling, average pooling, and maximum pooling. Minimum pooling is the process of identifying the value that is lowest from the pixel values inside the specified filter size, whereas maximum pooling is performed by choosing the highest value [33]. The idea behind average pooling is to divide the total number of pixel values inside the dimension of the filter region by the dimension of the filter window [34]. Figure 5 demonstrates the pooling process.

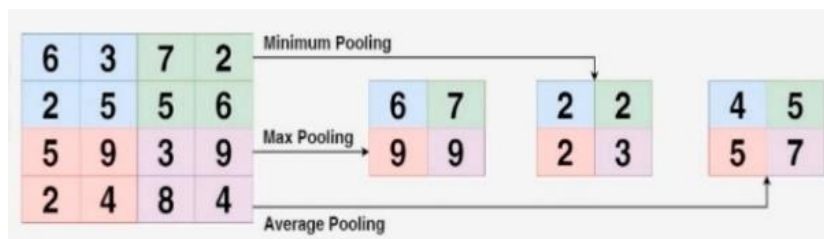


Figure 5. The pooling process [31]

2.4. Fully connected layer

Practically all types of neural network topologies use FC layers, which are among the most flexible layers. Every node is linked to every other node in the preceding and subsequent layers in this layer [35]. The major job of the layer is to convert the feature matrix to make the issue more pliable. Throughout this conversion, the total number of variables may rise, decrease, or remain constant. In every situation, the newly created dimensions are a linear mix of the dimensions from the preceding layer. Then, using an activation function, the additional dimensions are provided nonlinearity [36]. Figure 6. illustrates a six-dimensional space converted to a three-dimensional feature space by a FC layer.

FC layers allow for any type of interaction among input parameters. This behavior enables FC layers to acquire any function with enough width and depth [35]. Nevertheless, actual application has proven that such theoretical promise is frequently not fulfilled. To tackle this issue, scientists have developed particular layers such as recurrent and convolutional neural networks. These developed layers exploit inductive bias depending on the sequential or spatial arrangements of particular data sources, including text, videos, and images [36].

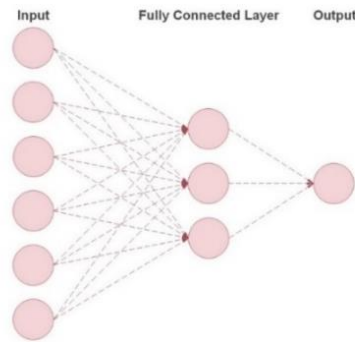


Figure 6. A systematic fully connected layer

2.5. Performance metrics

The main factor to consider during system training is accuracy. After which the entire training procedure is followed, this factor of the training images is recorded and plotted. Accuracy refers to how frequently a CNN model properly predicts objects, represented by the number of valid data to the total number of data as shown in (4). To verify the model's accuracy, the Keras assessment function was called on the constructed model, passing in the testing data as an input.

$$Accuracy = \frac{\text{Number of valid data}}{\text{Number of total data}} \quad (4)$$

In addition, other parameters are calculated to estimate the system efficiency such as precision, sensitivity or recall, and F1-score by the (5)-(7), [37].

$$Precision = \frac{TP}{TP+FP} \quad (5)$$

$$Recall = \frac{TP}{TP+FN} \quad (6)$$

$$F1 \text{ score} = 2 * \frac{Precision * recall}{Precision + Recall} \quad (7)$$

where: TP is the number of true positive
 FP is the number of false positive
 FN is the number of false negative

3. RESULTS AND DISCUSSION

This research aims to diagnose osteoporosis by classifying the X-ray images into three groups: healthy, actual osteopenia, and osteoporosis. The classification method of the designed CNN is represented by extracting the features of the collection images and classifying them automatically. Then the model intends to reduce human error and improve early disease detection rates.

Figure 7 illustrates the performance of the system in terms of accuracy with 30 epochs. Throughout the training period, an initial increasing tendency is noted. After the 13th epoch, the training line exceeds the validation line and stays continuously above it, but it is less noisy. Also, it can be observed that the validation line is more stable with higher values in the final phase, which means that the dynamic convolution increases the system's adaptability and validation efficiency. Anyway, the difference between the validation and train lines remains rather small, which indicates the efficiency of the designed system.

Regarding loss, during initial training, the suggested model experiences higher and more unstable loss. Demonstrating that the system is altered further during the preliminary phase, and the weights are regularly changed, as illustrated in Figure 8. With continued training, the validation line fluctuations can be observed to decrease as the loss values decrease significantly. At the final training phase, the validation line becomes more stable, and the gap with the train line widens somewhat.

Figure 9 displays the confusion matrix describing the relation between the actual values and the predicted values for the designed model. Besides providing knowledge about the classifier's shortcomings, it also displays any particular errors that may be appearing. It also assists in overcoming the problem of relying solely on classifier accuracy. The total accuracy of the system was (90.25 %) calculated based on the (4). Also,

the values of the calculated parameters are shown in the classification report in Table 2. The proposed model’s efficiency can be proven by comparing it with similar systems such as [38]–[41]. Table 3. illustrates that the proposed model performs better in accuracy than other works, which reveals a better diagnosis operation.

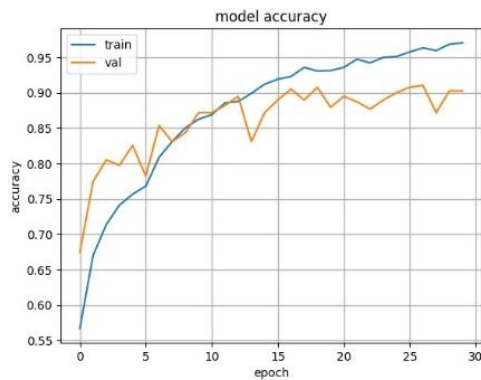


Figure 7. The accuracy of the designed CNN

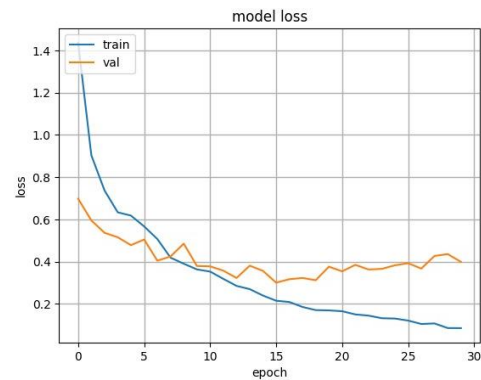


Figure 8. The loss of the designed CNN

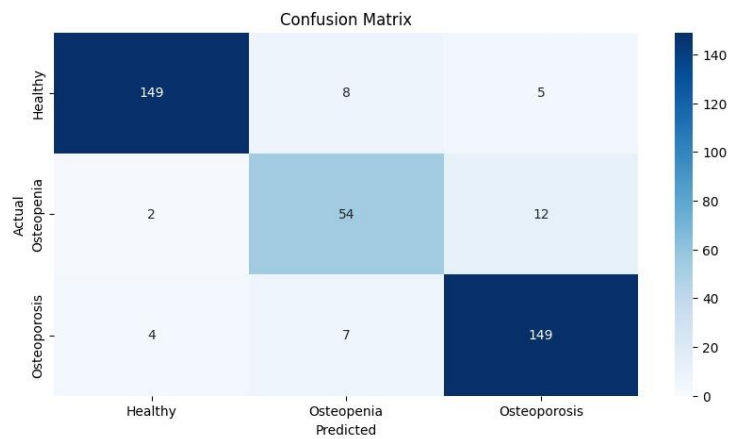


Figure 9. Confusion matrix relating to the dataset’s validation set

Table 2. Classification report

Class	Precision	Recall	F1-score
Healthy	0.961	0.919	0.939
Actual osteopenia	0.782	0.794	0.787
Osteoporosis	0.897	0.931	0.913

Table 3. Comparison of accuracy with other works

Reference	Title	Dataset	Method	Accuracy
[38]	Comparison of transfer learning model accuracy for osteoporosis classification on knee radiograph	240 X-ray images	GoogLeNet	90%
			VGG-16	87%
			ResNet-50	83%
[39]	Osteoporosis diagnosis in knee X-rays by transfer learning based on convolution neural network	381 knee X-ray images	AlexNet	90.91%
			ResNet	86.3%
			VggNet-19	84.2%
			VggNet-16	86.3%
[40]	Utilizing deep learning for osteoporosis diagnosis through knee X-ray analysis	1573 X-ray images	VGG 19	89%
[41]	Deep learning-based approaches for diagnosis and detection of osteoporosis using clinical data of CT and X-ray images	CT and X-ray the exact number of images not mentioned	Eight deep transfer learning approaches	VGG16 has the best accuracy of 82.73%
The proposed model	A CNN model for KOP Classification using X-ray images	1947 X-ray images	CNN	90.25%

4. CONCLUSION

The seriousness of KOP necessitates prompt diagnosis and treatment; nevertheless, depending on human specialists can prove costly and time-consuming. Making educated conclusions about images obtained from different patients is greatly aided by the assistance provided by visible AI. This paper produced an efficient CNN model design for classifying the available dataset. The main goals of the present research are to produce 1947 medical images of knee X-rays with 3 classes: healthy, actual osteopenia, and osteoporosis which are validated by multiple factors, and to suggest a deep learning method using an efficient CNN model to classify various levels of the disease. The suggested model produced encouraging outcomes and can assist doctors in diagnosing KOP in less time and at a reasonable cost. Further information can be gathered in the future, particularly from people who are osteoporotic and normal. In addition, in order to create a universal osteoporosis diagnosis method, we can determine the correlation between osteoporosis at the knee and osteoporosis at different locations. Furthermore, a system that uses clinical variables and imaging data to identify osteoporosis can be developed.

ACKNOWLEDGMENTS

The authors also extend their appreciation to the Department of Mechatronics Engineering, College of Engineering, University of Mosul, for their valuable assistance during the study.

FUNDING INFORMATION

Authors state no funding involved. The authors declare that this research was conducted without any external funding. All expenses were personally covered by the authors.

AUTHOR CONTRIBUTIONS STATEMENT

This journal uses the Contributor Roles Taxonomy (CRediT) to recognize individual author contributions, reduce authorship disputes, and facilitate collaboration.

Name of Author	C	M	So	Va	Fo	I	R	D	O	E	Vi	Su	P	Fu
Omar Khalid M. Ali	✓	✓	✓	✓	✓	✓	✓	✓	✓	✓	✓	✓	✓	✓
Abeer K. Ibrahim			✓	✓		✓		✓	✓		✓			✓
Bilal R. Altamer	✓	✓	✓		✓		✓	✓		✓	✓		✓	✓

C : **C**onceptualization

M : **M**ethodology

So : **S**oftware

Va : **V**alidation

Fo : **F**ormal analysis

I : **I**nterpretation

R : **R**esources

D : **D**ata Curation

O : **O**riginal Draft

E : **E**ditors

Vi : **V**isualization

Su : **S**upervision

P : **P**roject administration

Fu : **F**unding acquisition

CONFLICT OF INTEREST STATEMENT

Authors state no conflict of interest.

INFORMED CONSENT

We used the dataset available on the Kaggle website, so we have obtained informed consent from all individuals included in this study.

ETHICAL APPROVAL

The research related to human use has been complied with all the relevant national regulations and institutional policies in accordance with the tenets of the Helsinki Declaration and has been approved by the authors' institutional review board or equivalent committee.

DATA AVAILABILITY

The data that support the findings of this study are openly available in [Kaggle] at <https://www.kaggle.com/datasets/stevepython/osteoporosis-knee-xray-dataset> [21].

REFERENCES

- [1] O. Johnell and J. A. Kanis, "An estimate of the worldwide prevalence and disability associated with osteoporotic fractures," *Osteoporosis International*, vol. 17, no. 12, pp. 1726–1733, Oct. 2006, doi: 10.1007/s00198-006-0172-4.
- [2] H. Kato *et al.*, "Identification of ENPP1 haploinsufficiency in patients with diffuse idiopathic skeletal hyperostosis and early-onset osteoporosis," *Journal of Bone and Mineral Research*, vol. 37, no. 6, pp. 1125–1135, Dec. 2020, doi: 10.1002/jbmr.4550.
- [3] I. M. Wani and S. Arora, "Computer-aided diagnosis systems for osteoporosis detection: a comprehensive survey," *Medical & Biological Engineering & Computing*, vol. 58, no. 9, pp. 1873–1917, Sep. 2020, doi: 10.1007/s11517-020-02171-3.
- [4] H.-W. Chang, Y.-H. Chiu, H.-Y. Kao, C.-H. Yang, and W.-H. Ho, "Comparison of classification algorithms with wrapper-based feature selection for predicting osteoporosis outcome based on genetic factors in a taiwanese women population," *International Journal of Endocrinology*, vol. 2013, pp. 1–8, 2013, doi: 10.1155/2013/850735.
- [5] S. Gnudi, E. Sitta, and L. Lisi, "Relationship of body mass index with main limb fragility fractures in postmenopausal women," *Journal of Bone and Mineral Metabolism*, vol. 27, no. 4, pp. 479–484, Jul. 2009, doi: 10.1007/s00774-009-0056-8.
- [6] J. Kanis *et al.*, "A meta-analysis of previous fracture and subsequent fracture risk," *Bone*, vol. 35, no. 2, pp. 375–382, Aug. 2004, doi: 10.1016/j.bone.2004.03.024.
- [7] H. P. Dimai, "Use of dual-energy X-ray absorptiometry (DXA) for diagnosis and fracture risk assessment; WHO-criteria, T- and Z-score, and reference databases," *Bone*, vol. 104, pp. 39–43, Nov. 2017, doi: 10.1016/j.bone.2016.12.016.
- [8] WHO, "Assessment of fracture risk and its application to screening for postmenopausal osteoporosis," 1994.
- [9] Y. Chen, Y. Guo, X. Zhang, Y. Mei, Y. Feng, and X. Zhang, "Bone susceptibility mapping with MRI is an alternative and reliable biomarker of osteoporosis in postmenopausal women," *European Radiology*, vol. 28, no. 12, pp. 5027–5034, Dec. 2018, doi: 10.1007/s00330-018-5419-x.
- [10] A. D. Brett and J. K. Brown, "Quantitative computed tomography and opportunistic bone density screening by dual use of computed tomography scans," *Journal of Orthopaedic Translation*, vol. 3, no. 4, pp. 178–184, Oct. 2015, doi: 10.1016/j.jot.2015.08.006.
- [11] E. W. Gregg *et al.*, "The epidemiology of quantitative ultrasound: A review of the relationships with bone mass, osteoporosis and fracture risk," *Osteoporosis International*, vol. 7, no. 2, pp. 89–99, Mar. 1997, doi: 10.1007/BF01623682.
- [12] M. Kalbhor, S. V. Shinde, and H. Jude, "Cervical cancer diagnosis based on cytology pap smear image classification using fractional coefficient and machine learning classifiers," *TELKOMNIKA (Telecommunication Computing Electronics and Control)*, vol. 20, no. 5, pp. 1091–1102, Oct. 2022, doi: 10.12928/telkommika.v20i5.22440.
- [13] M. Ibrahim, M. Louie, C. Modarres, and J. Paisley, "Global explanations of neural networks," in *Proceedings of the 2019 AAAI/ACM Conference on AI, Ethics, and Society*, Jan. 2019, pp. 279–287, doi: 10.1145/3306618.3314230.
- [14] O. Loyola-Gonzalez, "Black-box vs. White-box: understanding their advantages and weaknesses from a practical point of view," *IEEE Access*, vol. 7, pp. 154096–154113, 2019, doi: 10.1109/ACCESS.2019.2949286.
- [15] S. Kajihara, S. Murakami, J. K. Tan, H. Kim, and T. Aoki, "Identify rheumatoid arthritis and osteoporosis from phalange CR images based on image registration and ANN," *ICIC Express Letters*, vol. 10, no. 10, pp. 2435–2440, 2016, doi: 10.24507/iceicel.10.10.2435.
- [16] K. Hatano, S. Murakami, H. Lu, J. K. Tan, H. Kim, and T. Aoki, "Classification of osteoporosis from phalanges CR images based on DCNN," in *2017 17th International Conference on Control, Automation and Systems (ICCAS)*, IEEE, 2017, pp. 1593–1596, doi: 10.23919/ICCAS.2017.8204241.
- [17] S. M. N. Fathima, R. Tamilselvi, M. P. Beham, and D. Sabarinathan, "Diagnosis of osteoporosis using modified U-net architecture with attention unit in DEXA and X-ray images," *Journal of X-Ray Science and Technology: Clinical Applications of Diagnosis and Therapeutics*, vol. 28, no. 5, pp. 953–973, Sep. 2020, doi: 10.3233/XST-200692.
- [18] B. Zhang *et al.*, "Deep learning of lumbar spine X-ray for osteopenia and osteoporosis screening: A multicenter retrospective cohort study," *Bone*, vol. 140, Nov. 2020, doi: 10.1016/j.bone.2020.115561.
- [19] N. Tecle, J. Teitel, M. R. Morris, N. Sani, D. Mitten, and W. C. Hammert, "Convolutional neural network for second metacarpal radiographic osteoporosis screening," *The Journal of Hand Surgery*, vol. 45, no. 3, pp. 175–181, Mar. 2020, doi: 10.1016/j.jhssa.2019.11.019.
- [20] C.-S. Ho *et al.*, "Application of deep learning neural network in predicting bone mineral density from plain X-ray radiography," *Archives of Osteoporosis*, vol. 16, no. 1, Dec. 2021, doi: 10.1007/s11657-021-00985-8.
- [21] StevePython, "Osteoporosis Knee Xray Dataset," 2021. <https://www.kaggle.com/datasets/stevepython/osteoporosis-knee-xray-dataset>
- [22] A. Krizhevsky, I. Sutskever, and G. E. Hinton, "ImageNet classification with deep convolutional neural networks," *Advances in neural information processing systems*, pp. 1–9, 2012.
- [23] H. Chung, S. J. Lee, and J. G. Park, "Deep neural network using trainable activation functions," in *2016 International Joint Conference on Neural Networks (IJCNN)*, Jul. 2016, pp. 348–352, doi: 10.1109/IJCNN.2016.7727219.
- [24] A. W. Sugiyarto, A. M. Abadi, and S. Sumarna, "Classification of heart disease based on PCG signal using CNN," *TELKOMNIKA (Telecommunication Computing Electronics and Control)*, vol. 19, no. 5, pp. 1697–1706, Oct. 2021, doi: 10.12928/telkommika.v19i5.20486.
- [25] Y. Lecun, L. Bottou, Y. Bengio, and P. Haffner, "Gradient-based learning applied to document recognition," *Proceedings of the IEEE*, vol. 86, no. 11, pp. 2278–2324, 1998, doi: 10.1109/5.726791.
- [26] K. Suzuki, "Overview of deep learning in medical imaging," *Radiological Physics and Technology*, vol. 10, no. 3, pp. 257–273, Sep. 2017, doi: 10.1007/s12194-017-0406-5.
- [27] S. Jain and A. O. Salau, "An image feature selection approach for dimensionality reduction based on kNN and SVM for Akt proteins," *Cogent Engineering*, vol. 6, no. 1, Jan. 2019, doi: 10.1080/23311916.2019.1599537.
- [28] M. A. A. Alobaidy, Z. M. Yosif, and A. M. Alkababchi, "Age-dependent palm print recognition using convolutional neural network," *Revue d'Intelligence Artificielle*, vol. 37, no. 3, pp. 795–800, 2023.
- [29] K. G. Kim, "Book review: Deep learning," *Healthcare Informatics Research*, vol. 22, no. 4, pp. 351–354, 2016, doi: 10.4258/hir.2016.22.4.351.
- [30] M. J. Mohammed, E. A. Mohammed, and M. S. Jarjees, "Recognition of multifold English electronic prescribing based on convolution neural network algorithm," *Bio-Algorithms and Med-Systems*, vol. 16, no. 3, Sep. 2020, doi: 10.1515/bams-2020-0021.
- [31] I. Pacal, D. Karaboga, A. Basturk, B. Akay, and U. Nalbantoglu, "A comprehensive review of deep learning in colon cancer," *Computers in Biology and Medicine*, vol. 126, Nov. 2020, doi: 10.1016/j.compbiomed.2020.104003.
- [32] A. Zafar *et al.*, "A comparison of pooling methods for convolutional neural networks," *Applied Sciences*, vol. 12, no. 17, Aug. 2022, doi: 10.3390/app12178643.
- [33] L. O. Lyra, A. E. Fabris, and J. B. Florindo, "A multilevel pooling scheme in convolutional neural networks for texture image

- recognition,” *Applied Soft Computing.*, vol. 152, p. 111282, 2024, doi: 10.1016/j.asoc.2024.111282.
- [34] E. A. Mohamed, T. Gaber, O. Karam, and E. A. Rashed, “A novel CNN pooling layer for breast cancer segmentation and classification from thermograms,” *PLOS ONE*, vol. 17, no. 10, Oct. 2022, doi: 10.1371/journal.pone.0276523.
- [35] M. S. Badar, *A guide to applied machine learning for biologists*. Cham: Springer International Publishing, 2023. doi: 10.1007/978-3-031-22206-1.
- [36] T. A. Kalaycı and U. Asan, “Improving classification performance of fully connected layers by fuzzy clustering in transformed feature space,” *Symmetry*, vol. 14, no. 4, Mar. 2022, doi: 10.3390/sym14040658.
- [37] R. Su, T. Liu, C. Sun, Q. Jin, R. Jennane, and L. Wei, “Fusing convolutional neural network features with hand-crafted features for osteoporosis diagnoses,” *Neurocomputing*, vol. 385, pp. 300–309, Apr. 2020, doi: 10.1016/j.neucom.2019.12.083.
- [38] U. B. Abubakar, M. M. Boukar, and S. Adeshina, “Comparison of Transfer Learning Model Accuracy for Osteoporosis Classification on Knee Radiograph,” in *2022 2nd International Conference on Computing and Machine Intelligence (ICMI)*, Apr. 2022, pp. 1–5. doi: 10.1109/ICMI55296.2022.9873731.
- [39] I. M. Wani and S. Arora, “Osteoporosis diagnosis in knee X-rays by transfer learning based on convolution neural network,” *Multimedia Tools and Applications*, vol. 82, no. 9, pp. 14193–14217, Apr. 2023, doi: 10.1007/s11042-022-13911-y.
- [40] M. Shen, “Utilizing deep learning for osteoporosis diagnosis through knee X-ray analysis,” in *Proceedings of the 2024 International Conference on Artificial Intelligence and Communication (ICAIC 2024)*, 2024, pp. 553–560. doi: 10.2991/978-94-6463-512-6_58.
- [41] S. Kaur, S. Kamboj, M. Kumar, A. Dagur, and D. K. Shukla, *Computational Methods in Science and Technology*. CRC Press, 2024. doi: 10.1201/9781003501244.

BIOGRAPHIES OF AUTHORS



Omar Khalid M. Ali    received the B.Eng. degree in Technical Computer Engineering from the Northern Technical University, Mosul, Iraq, in 2006, and the Master’s degree in Technical Computer Engineering from the same university in 2020, and now he is a Ph.D. student at University Sains Malaysia (USM), Penang, Malaysia. He is currently an assistant lecturer. He works at the Construction and Project Department at the University of Mosul, where he is also a lecturer in the Mechatronics Department, Faculty of Engineering at the University of Mosul. His current research interests include AI, IoT and computer networks. He can be contacted at email: omar.khalid@uomosul.edu.iq.



Abeer K. Ibrahim    received a B.Eng. degree in Computer Engineering from the University of Mosul, Mosul, Iraq, in 2007, and a Master’s degree in Computer Engineering science from the Northern Technique University/Computer Technique Engineering, Iraq, in 2022. She is currently an assistant lecturer in the Department of Environmental Engineering, at the University of Mosul. Her current research interests include artificial intelligence and deep learning. She can be contacted at: abeer.khalil@uomosul.edu.iq.



Bilal R. Altamer    received the B.Eng. degree Technical Computer Engineering from the Northern Technical University, Mosul, Iraq, in 2007, and the Master’s degree in Technical Computer Engineering from the same university in 2020, and now he is a Ph.D. student at University Sains Malaysia (USM), Penang, Malaysia. He is currently an assistant lecturer. He works at Mosul University Presidency where he is also a lecturer in the Mechatronics Department, Faculty of Engineering at the University of Mosul. His current research interests include IoT and deep learning and machine learning. He can be contacted at email: bilal.altamer@uomosul.edu.iq.